Electronic Journal of Structural Engineering

Original Article

Cite this: DOI:10.56748/ejse.24605

Received Date: 01 March 2024
Accepted Date: 27 October 2024

1443-9255
https://ejsei.com/ejse

Analyzing the Impact of Multiple Foundation Stiffness Correlations on the Natural Frequency of Offshore wind turbines

Laib Abdelghani [a], Bakhti Rachid [a,b], Benahmed Baizid [c*]

[a] Department of Civil Engineering, Faculty of Science and Applied Science, University of Bouira, Bouira, Algeria
[b] Laboratory of TPiTe National School of Build and Ground Works Engineering ENSTP, Algiers, Algeria
[c] Civil Engineering Department, Development laboratory in mechanics and materials, university of Djelfa, Algeria
*Corresponding author: benahmed.tp@univ-djelfa.dz

Abstract

The analysis of wind turbine behavior should avoid unplanned resonance, as it can increase fatigue damage. It is essential to rigorously evaluate the natural frequency of wind turbines in the initial design stage. This estimation can be done through two steps, the first one is the computing of the fixed base natural frequency of the wind turbine. The second is the estimation of the foundation stiffness effect. This paper examines the error margin of four correlations of foundation stiffness namely Randolph, Davies and Budhu, DNV, and Higgins in the estimation of the natural frequency of wind turbines. The fixed base natural frequency was estimated in this paper using a special-purpose finite element computer program called TurbiSoft through beam and volume elements. A reference 5.0 MW offshore wind turbine and 9 other turbines from different wind farms have been analyzed. For the fixed base natural frequency, obtained results demonstrate the reliability of the finite element program TurbiSoft through an error margin between 1-4% for the reference 5.0 MW offshore wind turbine. For the natural frequency of the whole system, the estimated error marking was between 9-20% which is an important value. This significant error is attributed to the low accuracy of these four correlation formulas for predicting the foundation flexibility contribution. The results from the four correlation formulas used are quite similar, with a difference in the error margin of less than 1%. However, the largest error margins are observed with the Higgins formula, which has been originally developed for short monopiles, even though the analyzed monopiles can be considered short, with monopile slenderness ratios less than 8.

Keywords

Finite element analysis, Natural frequency, Wind turbines, Tapered tower, Beam element, Foundation stiffness

1. Introduction

Numerous wind energy developments have been the subject of research projects since the 1973 oil crisis. The cost optimization of renewable energy has reached historic levels. For example, wind turbines are now able to produce competitively priced electricity compared to fossil fuels. It is well known that the height and the weight of wind turbine increase significantly its cost and makes the tower relatively flexible. Thus, the analysis of wind turbine behavior should avoid unplanned resonance, as it can increase fatigue damage (Arany et al., 2015). In addition to dynamic excitations from wind loading, the rotor nacelle assembly (RNA) is the main source of dynamic excitation of the wind turbines. Modern wind turbines can have constant (fixed 1P) or variable (1P range) rotational speed machines. These last ones have 1P rotational frequency bands and blade passing frequency bands (2P/3P) which may lead to unplanned resonance and must be avoided in design of support structure.

Tempel and Molenaar (2002) proposed three possible ranges in which the predominant frequency of the wind turbines should lie according to the stiffness of the foundation: the first one is soft-soft system: the natural frequency can be less than (1P). In this case, the structure is very flexible. This design is practically impossible to achieve for fixed structures (Arany et al., 2016). The second range is soft-stiff system: the natural frequency can be between (1P) and (3P) for a three bladed rotor (2P for turbines built with two rotor blades), this is the typical range for the best possible design. The last range is stiff-stiff system: the natural frequency can be greater than (3P). In this case, the structure is very stiff. This design is uneconomic.

Since monopiles are commonly used as support foundations for wind turbines, the behavior of wind turbine structures, which typically have highly flexible towers, is significantly affected by the foundation flexibility (Adhikari & Bhattacharya, 2012). Designing foundations for such structures is crucial in the dynamic analysis, and foundation flexibility cannot be neglected, especially when the wind turbine is founded on a soft soil (Ko, 2020). The overall foundation stiffness depends on both the stiffness of the soil and the structural elements of the foundation. Therefore, accurate soil stiffness values should be derived for the dynamic analysis of the wind turbine structures. In addition, it has been recognized that the foundation system can be commonly represented by three coupled springs: lateral, rocking, and cross-coupling (Bakhti et al., 2023).

Because the rigidity of the wind turbine structure is influenced by its supporting foundation, the predominant frequency of the wind turbines may be evaluated via the estimation of the fixed base natural frequency of the tower. Then, the foundation and soil–structure interaction effects are introduced by multiplying the fixed base value with non-dimensional factors. In this framework, several analytical models (Arany et al., 2015, 2016; Adhikari & Bhattacharya, 2012; Rong et al., 2017) as well as numerical approaches based on the finite element method (Bakhti et al., 2023; Xu et al., 2020; Alkhoury et al., 2021; A. Abdullahi & Y. Wang, 2021; Park et al., 2022; Steinacker et al., 2022; Shi et al., 2022; Huang, 2022) have been proposed to predict the fixed base natural frequency and the contribution of the supporting foundation. The major issue for the calculation of the foundation stiffness is the lack of information and data availability of site material properties. Analytical correlation formulas of the foundation stiffness proposed in the literature (DNV-OS-J101, 2014; Randolph, 1981; Davies & Budhu, 1986; Higgins et al., 2013) may represent an alternative solution to this issue.

The aim of this paper is the investigation into the effect of the finite element models on the wind turbine natural frequencies and the assessment of the validity of some analytical formulas proposed in the literature regarding the foundation flexibility contribution. A finite element modeling of wind turbine towers has been developed to calculate their natural frequencies using multiple finite elements. In order to select the most suitable solution, linear beam element (2 nodes), linear axisymmetric element (4 nodes) and quadratic axisymmetric element (8 nodes) are used for calculating the fixed base natural frequency of the tower. A finite element computer code was proposed especially for this study under the name "TurbiSoft" in which natural frequencies and normal modes of fixed base wind turbines are provided. The foundation flexibility effect has been investigated through the analytical formulas proposed in the literature for lateral stiffness, rotational stiffness and cross coupling stiffness. For the validation process, the proposed solution was applied for nine offshore wind turbines from seven wind farms to get the variation range in the natural frequency.

2. Closed-form solutions for the natural frequency of OWT

Several analytical analyses of the natural frequency of wind turbines are carried out in the literature based on the Euler–Bernoulli and Timoshenko beam theories. In these analyses, the wind turbine is represented as fixed base cantilever beam with top mass equivalent to the RNA mass. Three coupled springs (lateral, rocking and cross-coupling) are commonly used to model the foundation system. The influence of this foundation on the natural frequency of the total structure is introduced through non-dimensional factors.

Vught (2000) used a simple idea to estimate the fixed base natural frequency of wind turbines where the foundation system has been ignored and the wind turbine is considered as a flagpole of length L, flexural rigidity $E_T I_T$, global mass $m_T^{'}$ and a top mass m_{RNA} equal to the total weight of the RNA (Fig. 1.c). The first natural frequency is derived as follows:

$$f_{FB,T} = \frac{1}{2\pi}\sqrt{\frac{3.04\,E_T I_T}{L^3\left(m_{RNA}+0.227 m_T^{'}\right)}} \quad (1)$$

Based on the same hypothesis, another expression provided by Blevins (2001):

$$f_{FB,T} = \frac{1}{2\pi}\sqrt{\frac{3\,E_T I_T}{L^3\left(m_{RNA}+\frac{33}{144} m_T^{'}\right)}} \quad (2)$$

Based on a Euler-Bernoulli beam-column with elastic end supports, Adhikari and Bhattacharya (2012) proposed a simplified approach for the vibration analysis of wind turbines with and without the foundation effect. An analytical expression of the natural frequency of the system has been derived. Their analytical results showed that the natural frequency of the turbine tower decreases as the stiffness of the foundation decreases and the axial load increases. Rong et al. (2017) provided a physical derivation of the first natural frequency of wind turbines supported by monopile based on Rayleigh's method. Their expression contains only physical parameters, and it is reduced to the equation of Blevins (2001) for turbines modelled as Euler-Bernoulli beam with a top mass.

Most of analytical expressions of natural frequency of the wind turbines are developed only for simple models in which the turbine is idealized as a beam with a uniform cross section and cannot be reliably extrapolated to other different turbines that have generally tubular and conical shape with irregular wall thickness; their range of applicability may be limited. On the other hand, many researchers have proposed analytical models for wind turbines with irregular shapes. Arany et al. (2016) proposed a methodology to obtain the predominant frequency of an offshore wind turbine supported by a monopile by multiplying the fixed base wind turbine natural frequency by two factors to consider the flexibility of the substructure and the compliance of the foundation. The studied wind turbines had tapered towers with diameters increasing from the top to the bottom. Also, the wall thickness of the towers decreases with height. The shape of the tapered tower is reduced to a constant wall thickness tower and constant diameter D_T (fig. 1):

$$D_T = \frac{D_{top}+D_{bottom}}{2} \quad (3)$$

Their expression for the fixed base natural frequency of the wind turbine and the substructure system is written as:

$$f_{FB} = \frac{1}{2\pi}\sqrt{\frac{3\,E_T I_T}{L^3\left(m_{RNA}+\frac{33}{140} m_T^{'}\right)}}\sqrt{\frac{1}{1+(1+\psi)^3\chi-\chi}} \quad (4)$$

Where: $\psi = \frac{L_S}{L_S}, \chi = \frac{E_T I_T}{E_S I_S}$

Yung-Yen Ko (2020) proposed a solution of wind turbines natural frequencies with tapered towers founded on a rigid-base condition as:

$$f_{RB(tapered)} = \frac{1}{2\pi}\sqrt{\frac{K_{T(tapered)}}{\left(m_{RNA}+\alpha\, m_{T(tapered)}\right)}} \quad (5)$$

Where: $K_{T(tapered)}$ is the lateral stiffness of the tower and $m_{T(tapered)}$ is its mass. In this equation, the wind turbines considered were those starting from the tower base. In the case where the substructure is included, the total structure becomes more flexible because it has an additional length. The natural frequency of the wind turbine including the additional length of the substructure is written as follows:

$$f_{RB(tapered+ss)} = \frac{1}{2\pi}\sqrt{\frac{K_{T(tapered+ss)}}{\left(m_{RNA}+\alpha\, m_{T(tapered+ss)}\right)}} \quad (6)$$

Where $m_{T(tapered+ss)}$ and $K_{T(tapered+ss)}$are the mass and the lateral stiffness of the tower including the substructure, respectively.

You et al. (2022) suggested an analytical expression for the natural frequency of the fixed base offshore wind turbine taking into account the seawater inside the substructure:

$$f_{RB(tapered+ss+\omega)} = \frac{1}{2\pi}\sqrt{\frac{K_{T(tapered+ss)}}{\left(m_{RNA}+\alpha\, m_{T(tapered+ss)}+\alpha_\omega m_\omega\right)}} \quad (7)$$

Where m_ω is the weight of the water existing inside the monopile, α_ω is a mass ratio for including the distance of inner fluid from the mudline than RNA.

The authors (You et al., 2022) indicated that the predominant frequency estimation expression including the inner fluid has a smaller error rate.

Many of these analytical models estimate the natural frequency of wind turbines by adopting many simplified assumptions as the idealization of the tubular and conical tower of irregular wall thickness with an equivalent diameter and constant wall thickness. In fact, these assumptions, which provide quick and easy solutions, are the sources of uncertainties and influence the accuracy of the final natural frequency prediction. Therefore, the idealization of wind turbines with complex shapes by the Euler Bernoulli beam becomes more difficult and seems not adapted to the physical realities of the design.

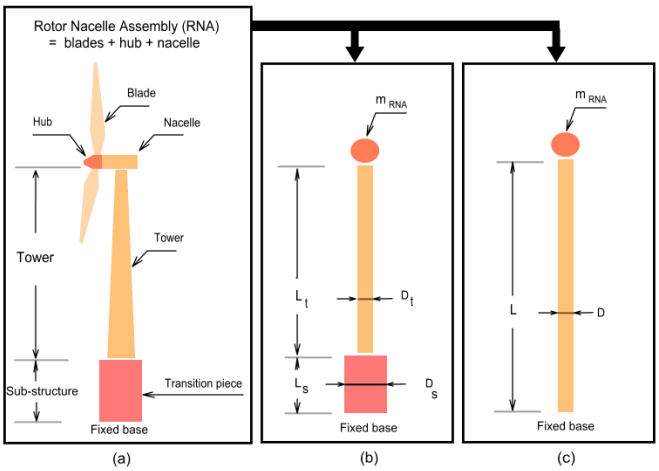

Fig. 1 Analytical model (a): Main components (b): Arany model (c): beam model

3. Finite element estimation of the OWT natural frequency

Many researchers have developed numerical approaches for estimating the natural frequency and structural modes of wind turbines. These approaches, typically based on high-fidelity finite element analysis, have the potential to produce more reliable results for wind turbines with complex shapes.

In this context, Xu et al. (2020) provided a finite element analysis for modeling the structural behaviors of the offshore wind turbine founded on monopile in sand deposits using the simulation ANSYS program. The tower and monopile are both simulated by element beam that is based on Timoshenko theory that takes into account the shear-deformation. The mass at the top is simulated by element mass which can have six degrees of freedom. Their obtained results indicated that the difference between the test result of the natural frequency and that estimated by the finite element analysis is about 1.7%. To achieve a structural analysis of the wind turbine installed in parked condition, Alkhoury et al. (2021) developed a 3D solid finite element model of offshore wind turbine using the commercial finite element code Abaqus. The different parts of the tower were modelled using 8-node layered shell elements. Solid elements are used to model the monopile to include the soil-monopile interaction. The material properties of the tower and the monopile were supposed to have an elastic isotropic behavior. Obtained results revealed that the more detailed and specific modeling of the grouted connection between the base of tower and the monopile does not have a meaningful influence on the value of natural frequency of the whole system.

Abdullahi and Wang (2021) developed a 2D finite element model of laboratory offshore wind turbine using some parameters of soil-structure interaction in the simulation ANSYS program in which the tower and monopile are modelled by a beam element. They pointed out that a difference of only 0.018% for natural frequencies is observed compared to the experimental values. You et al. (2022) developed a 3D finite element model using the simulation ANSYS program to analyze the variation in the natural frequency of offshore wind structures taking into account the interaction between the fluid and structure. The elements of structure were modelled as 20-node solid element which has a quadratic displacement behavior. Each node has three degrees of freedom. Obtained results indicated that the difference between the estimated predominant frequency of the studied wind turbine with rigid base and other studies was less than 4%, taking into account only the tower's shape. To predict the degradation of the dynamic characteristics of an offshore wind turbine with tripod substructure, Park et al. (2022) implemented a 3D finite element model of a 3-MW WinDS3000 TC-2 wind turbine (Seo et al., 2020). Triangular shell elements were used for the modeling of the tower and substructure. Their study showed that the natural frequencies of wind turbines using measured dynamic parameters of the structure could be predicted accurately using the proposed finite element model.

Steinacker et al. (2022) presented finite element approach for flexible substructures of offshore wind turbines by modifying the OpenFAST-SubDyn approach to determine natural frequencies. Flexible bodies of finite element model were integrated into a simulation tool for the equation of motion of the low order wind turbine. Obtained results indicated that coupled and uncoupled natural frequencies showed differences of less than 3 %. Shi et al. (2022) developed a 3D finite element analysis of 5MW wind turbine implemented in the general finite element program of Abaqus. The tower is modeled as tapered beam element with annular section, while beam element with constant and annular section is used to model the substructure. Results of their analysis demonstrated that the numerical model implemented in Abaqus provides a reliable estimate of the natural frequency of wind turbines. Nevertheless, natural frequencies derived in the time domain using the free and open-source code FAST are higher than those estimated by their numerical model. Bakhti et al. (2023) suggested considering the structure turbine foundation as an axisymetric problem with non axisymetric loads for simulating the natural frequency of the whole system. In their study, the four-node and the eight-node ring elements have been used to simulate the system turbine-foundation. Their results indicated that the soil profile variation effects on the natural frequency estimation are not as important as the interaction soil–pile state.

For simulating the behavior of wind turbines and their natural frequencies, different finite element models (beam, shell, etc.) are used in the presented finite element analyses. The DNV code (2014) suggested several elements for the offshore wind turbines that are summarized in Table 1.

Table 1. Elements proposed by DNV to analyze wind turbines (DNV-OS-J101, 2014)

Element type	Description
BEAM2D	Beam element, 2 nodes per element, 3 DOF per node, u_x,u_y and θ_z
PLANE2D	Membrane element, 4 nodes per element, 2 DOF per node, u_x andu_y
TRIANG	Membrane element, 3 nodes per element, 2 DOF per node, u_x andu_y
SHELL3	Shell element, 3 nodes per element, 6 DOF per node
SOLID	Solid element, 8 nodes per element, 3 DOF per node, u_x, u_y and u_z
TETRA4	Solid element, 4 nodes per element, 3 DOF per node, u_x, u_y and u_z
TETRA4R	Solid element, 8 nodes per element, 6 DOF per node

4. The foundation stiffness correlation

The foundation of the wind turbine refers to the segment of the support structure that interfaces with the ground. The foundation stiffness depends on both the strength and stiffness of the soil, as well as on the elements of structural foundation. The foundations of the wind turbines must resist cyclic lateral loads induced by waves, winds, and earthquakes. These repeated loads cause a change in soil properties leading to a gradual reduction in pile capacity (Owji et al., 2023). This decrease in pile capacity can change the natural frequency of the whole system, leading to structural resonance and potential fatigue damage. The foundation system is considered to have a linear behavior. Thus, three coupled springs can be used to model the foundation. The major issue for the calculation of the foundation stiffness is the lack of information and data availability of site material properties. Several approximate analytical formulas have been proposed in the literature for the stiffness of the foundation which is a key parameter in the calculation of the natural frequency of the total structure. Most of these correlations of the foundation stiffness, which depend on monopile-soil stiffness ratio (E_P/E_s or E_P/G_s) and the monopile slenderness ratio (L_P/D_P), presented closed form solutions for the foundation flexibility coefficients.

Randolph (1981) carried out a parametric study on the response of the piles under lateral loading using the finite element method in which the soil is modelled as an elastic continuum with a linearly varying soil modulus. The results were presented as a formula for lateral stiffness K_L, rotational stiffness K_R and cross coupling stiffness K_{LR} of flexible piles subjected to lateral loads, where bending moments and the induced deformations were confined to the upper part of the pile. The response of the pile is not significantly affected by its overall length:

$$K_L/(E_{sD}.D) = 1.751(E_P/E_{sD})^{0.333}$$
$$K_{LR}/(E_{sD}.D^2) = -0.506(E_P/E_{sD})^{0.555}$$
$$K_R/(E_{sD}.D^3) = 0.248(E_P/E_{sD})^{0.777} \quad (8)$$

Where E_P the monopile material Young's modulus, and E_S is the soil modulus. E_{sD} is the soil modulus estimated at z depth equal to monopile diameter D.

Its formula presented the quantification of the interaction between neighboring piles effects, from which the behavior of groups of piles subjected to lateral loads can be derived. Davies and Budhu (1986) presented a study of the non-linear behavior of laterally loaded single piles embedded in heavily over-consolidated clays, derived from a boundary element analysis where the soil is modelled as an elastic continuum and the pile as an elastic flexural member. They discussed the influence of soil shear strength on both deformations and bending moments and proposed the following formula for the foundation idealization (as three springs):

$$K_L/(E_{sD}.D) = 0.734(E_P/E_{sD})^{0.333}$$
$$K_{LR}/(E_{sD}.D^2) = -0.270(E_P/E_{sD})^{0.555}$$
$$K_R/(E_{sD}.D^3) = 0.173(E_P/E_{sD})^{0.777} \quad (9)$$

Using the P-Y curves method that represents the nonlinear relationship between pile deflection (Y) and soil reaction (P), the DNV code for offshore wind turbines (DNV-OS-J101, 2014) reported the following expressions of the foundation stiffness:

$$K_L/(E_{sD}.D) = 0.600(E_P/E_{sD})^{0.350}$$
$$K_{LR}/(E_{sD}.D^2) = -0.170(E_P/E_{sD})^{0.600}$$
$$K_R/(E_{sD}.D^3) = 0.140(E_P/E_{sD})^{0.800} \quad (10)$$

Using the Fourier FEM, Higgins et al. (2013) analyzed the laterally loaded piles with different lengths and boundary conditions embedded in elastic media with constant and linearly varying modulus. The pile responses were obtained to be functions of the pile slenderness ratio L_P/D_P. Based on their parametric study of variables governing the pile behavior, algebraic equations describing the soil stiffness were proposed:

$$K_L/(E_{sD}.D) = 0.929(L_P/D_P)^{2.041}$$
$$K_{LR}/(E_{sD}.D^2) = -0.633(L_P/D_P)^{3.061}$$
$$K_R/(E_{sD}.D^3) = 0.672(L_P/D_P)^{3.941} \quad (11)$$

Where L_P is the length of the monopile and D_P is its diameter.

The correlations of the foundation stiffness mentioned above are used in this paper for the modelling of the foundation system with three coupled springs (K_L,K_R,K_{LR}) as non-dimensional coefficients using the length of the tower L_T and the equivalent bending stiffness of the tapered tower EI_η (Arany et al., 2016):

$$\eta_L = \frac{K_L L_T^3}{EI_\eta} \quad \eta_{LR} = \frac{K_{LR} L_T^2}{EI_\eta} \quad \eta_R = \frac{K_R L_T}{EI_\eta} \quad (12)$$

The equivalent bending stiffness of the tapered tower is calculated as follows:

$$\mathrm{EI}_\eta = \mathrm{EI}_T \times f(q) \quad (13)$$

Where EI_T is bending stiffness at the top of the tower.

$$f(q) = \frac{1}{3} \times \frac{2q^2(q-1)^3}{2q^2 \ln q - 3q^2 + 4q - 1} \quad (14)$$

Where q is the ratio of the bottom and top tower diameters $q = D_b/D_t$.

The foundation system effects on the natural frequency of the whole structure are included by means of the two foundation flexibility factors C_R and C_L (non-dimensional factors) which are multiplied by the fixed base natural frequency f_{FB}:

$$C_R = 1 - \frac{1}{1 + a\left(\eta_R - \frac{\eta_{LR}^2}{\eta_L}\right)} \quad C_L = 1 - \frac{1}{1 + b\left(\eta_l - \frac{\eta_{LR}^2}{\eta_R}\right)} \quad (15)$$

Where a and b are constants equal to 0.6 and 0.5, respectively.

The natural frequency of the whole system of the wind turbine f can be calculated using the simple formula provided by Arany et al. (2016):

$$f = C_R C_L f_{FB} \quad (16)$$

5. Method

Concerning the modelling of the fixed base wind turbines in this study, two different finite element approaches are considered. In the first one, the wind turbine is considered as a beam with top mass, in which the finite element models are made of 2-node beam elements. In the second one, the wind turbine is considered as an axisymmetric solid element with non-axisymmetric loads where two elements have been used which are the 4-node and 8-node rings elements.

For the estimation of the natural frequencies, the process begins with the discretization of the structure followed by the estimation of the elementary matrices and load vector. After that, we need to compute the global mass and stiffness matrices. The next step is the boundary condition incorporation and the solution computation by solving the equation:

$$det([K] - w^2[M]) = 0 \quad (17)$$

5.1 Beam element

In this section, the wind turbine is considered as a beam with top mass, in which the finite element models are made of 2-node beam elements. The conical part of the wind turbine is divided into "N" uniform round tubular segments, where each segment "k" has an effective diameter (Fig. 2.b) given by:

$$D_k = D_{bottom} + \left(D_{top} - D_{bottom}\right) \sum_{i=1}^{k} \frac{L_i}{L_t} \quad (18)$$

Where L_t is the height of the conical part, L_i is the height of the segment

"i", $D_{top}$is the diameter of the top of the conical part, and D_{bottom} is the diameter of the bottom of the conical part.

For a beam of length L, mass M and a flexural rigidity EI, the stiffness and the lumped mass matrices are, respectively, presented by:

$$[K]_e = \frac{EI}{L^3}\begin{bmatrix} 12 & 6L & -12 & 6L \\ 6L & 4L^2 & -6L & 2L^2 \\ -12 & -6L & 12 & -6L \\ 6L & 2L^2 & -6L & 4L^2 \end{bmatrix} \quad (19)$$

$$[m]_e = m\begin{bmatrix} \frac{1}{2} & 0 & 0 & 0 \\ 0 & 0 & 0 & 0 \\ 0 & 0 & \frac{1}{2} & 0 \\ 0 & 0 & 0 & 0 \end{bmatrix} \quad (20)$$

Using equation (17), the fixed base natural frequency is calculated through the JK method proposed by Kaiser (1972), a procedure for determining the eigenvectors and eigenvalues of a real symmetric matrix.

5.2 The axisymmetric model for the wind turbines

As demonstrated by the authors in (Bakhti et al., 2023), the Wind turbine can be modelled perfectly using the axisymmetric element with non-axisymmetric loads. In this study, each of the 4-node and the 8-node ring elements was used for the modelling of the tower (Fig. 3 and 4). The origin of the element is in its centroid. Each node of the ring element has three degrees of freedom.

For an axisymmetric solid with non-axisymmetric loading, the stiffness matrix can be determined as follows:

$$[K]_i^n = \int_A \int_{-\pi}^{\pi} [B]_i^{nT}[D][B]_i^n r.dr.dz.d\theta \quad (21)$$

Where $[D]$ represents the materiel property and takes the following form:

$$[D] = \frac{E}{(1+\nu)(1-2\nu)}\begin{bmatrix} (1-\nu) & \nu & \nu & 0 & 0 & 0 \\ \nu & (1-\nu) & \nu & 0 & 0 & 0 \\ \nu & \nu & (1-\nu) & 0 & 0 & 0 \\ 0 & 0 & 0 & (0.5-\nu) & 0 & 0 \\ 0 & 0 & 0 & 0 & (0.5-\nu) & 0 \\ 0 & 0 & 0 & 0 & 0 & (0.5-\nu) \end{bmatrix} \quad (22)$$

With E is the elastic modulus and ν is the poisson's ratio.

$[B]^n$is associated with "n" harmonic, it is computed as follows:

$$\left[B_j^n\right] = \begin{bmatrix} \frac{\partial N_j}{\partial r}cosn\theta & 0 & 0 \\ 0 & \frac{\partial N_j}{\partial z}cosn\theta & 0 \\ \frac{N_j}{r}cosn\theta & 0 & \frac{nN_j}{r}cosn\theta \\ \frac{\partial N_j}{\partial z}cosn\theta & \frac{\partial N_j}{\partial r}cosn\theta & 0 \\ 0 & \frac{nN_j}{r}sinn\theta & \frac{\partial N_j}{\partial z}sinn\theta \\ -\frac{nN_j}{r}sinn\theta & 0 & \left(\frac{\partial N_j}{\partial r}-\frac{N_j}{r}\right)sinn\theta \end{bmatrix} \quad (23)$$

The trigonometric functions integration provides a value of π. So, the stiffness matrix becomes:

$$\left[K\right]_i^n = \pi\int_A \left[B\right]_i^T\left[D\right]\left[B\right]_i r\ .dr.dz \quad (24)$$

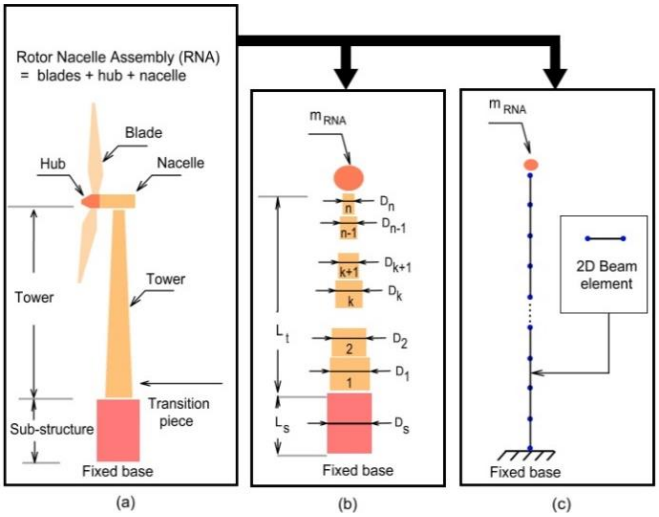

Fig. 2 The beam model: (a) Main components, (b) modelling of the conical part, (c) wind turbine mesh

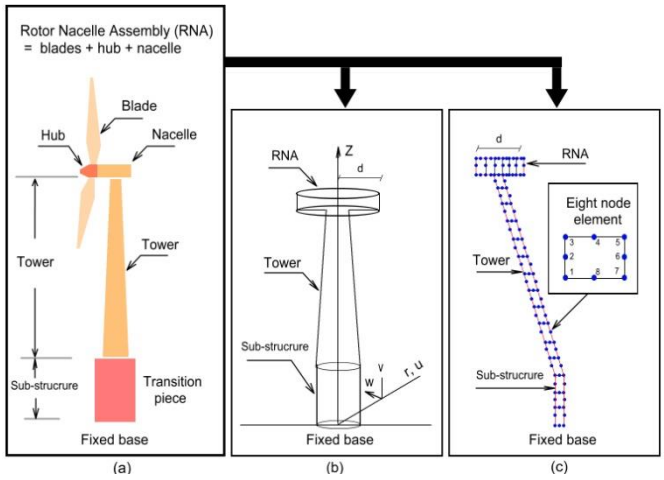

Fig. 3 The axisymmetric model of wind turbine: (a) Main components, (b) axisymmetric model, (c) wind turbine mesh

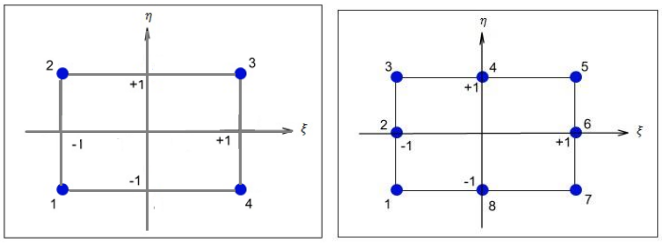

Fig. 4 Four-node and Eight-node elements

Where $[D]$ is matrix given by equation (22), and $[B]_i$ is defined as:

$$[B]_i = [\partial].[N]_i \quad (25)$$

The operator matrix $[\partial]$ is written as:

$$[\partial] = \begin{bmatrix} \frac{\partial}{\partial r} & 0 & 0 \\ \frac{1}{r} & \frac{1}{r}\frac{\partial}{\partial \theta} & 0 \\ 0 & 0 & \frac{\partial}{\partial z} \\ \frac{\partial}{\partial z} & 0 & \frac{\partial}{\partial r} \\ \frac{1}{r}\frac{\partial}{\partial \theta} & \frac{\partial}{\partial r}-\frac{1}{r} & 0 \\ 0 & \frac{\partial}{\partial z} & \frac{1}{r}\frac{\partial}{\partial \theta} \end{bmatrix} \quad (26)$$

The shape functions matrix $[N]_i$ is given by:

$$\left[N\right]_i = \begin{bmatrix} N_1 & 0 & 0 & \cdots \\ 0 & N_1 & 0 & \cdots \\ 0 & 0 & \underbrace{N_1}_{1} & \underbrace{\cdots}_{2,3,\ldots EN} \end{bmatrix} \quad (27)$$

Where, EN is 4 for a 4-node ring and 8 for an 8-node ring.

The solution of the equation (17) can be obtained by two methods, the first one using the consistent mass matrix, the second using the lumped mass matrix. This latter is adopted due to its reduced computational cost. Using the diagonal matrix, the consistent mass matrix is transformed into a lumped mass matrix. The consistent mass matrix of the element I associated with "n" harmonic may be calculated as:

$$\left[m\right]_i^n = \int_{A-\pi}^{\pi}\int \rho\left[N\right]_i^{n^T}\left[N\right]_i^n r.dr.dz.d\theta \quad (28)$$

In which $[N]_i^n$ is the shape function matrix associated with "n" harmonic, ρ is the mass density. Using the same process as stiffness matrix, the consistent mass becomes:

$$\left[m\right]_i^n = \pi\rho\int_A \left[N\right]_i^T\left[N\right]_i r\ .dr.dz \quad (29)$$

Where $[N]_i$ is the shape function matrix of element I, its expression is given by equation (27).

5.3 TurbiSoft

For calculating the fixed base natural frequency of the wind turbines, the above-described finite element solution is coded in a special-purpose computer program TurbiSoft written and compiled in Microsoft's visual studio community 2022 using visual basic.NET (Fig. 5). The number of

nodes required for the discretization is significantly reduced when using the axisymmetric approach. The discretization is applied only on the rotary plan area, resulting in a reduction of the size of both the stiffness and mass matrices. Thus, the computational cost is considerably reduced.

TurbiSoft can calculate the natural frequency and simulate the behavior of OWTs under static loading using input data such as the tower's geometry, tower's mechanical properties, and properties of the nacelle. To test the functioning of TurbiSoft program and to demonstrate if its requirements are implemented correctly, the estimated fixed base natural frequencies were compared with analytical and numerical solutions from the literature.

6. Results and discussion

To demonstrate the effect of the used finite element models on the natural frequency of wind turbines, the proposed finite element solution implemented in TurbiSoft is applied to a reference 5.0 MW offshore wind turbine model of the National Renewable Energy Laboratory (NREL). The results of the proposed solution are compared with those of other studies (Ko, 2020; You et al., 2022). The characteristics for dimensions and the mass of the conical tower are presented in table 2. Further details on the reference 5.0 MW offshore wind turbine can be found in You et al. (2022). Table 3 presents the results of the proposed solution in terms of the natural frequency compared with those of Yung-Yen Ko (2020) and You et al. (2022) for the fixed base model of the NREL turbine. The natural frequency of the fixed base model estimated by the two proposed approaches is about 1-4% from that of other studies. The present solution shows good accuracy in terms of results. It can be seen that there is no significant difference (less than 1%) between the natural frequency values estimation by the two proposed approaches (volume and beam elements).

Table 2. Input parameters for the NREL 5 MW reference wind turbine (You et al., 2022)

Contents	value
Length of tower (m)	87.6
Outer diameter of tower top (m)	3.87
Thickness of tower top (m)	0.019
Outer diameter of tower bottom (m)	6.0
Thickness of tower bottom (m)	0.027
Total weight of RNA(Kg)	350 000
CM height from tower top of RNA (m)	1.817
Material Young's modulus (Gpa)	210

To check the accuracy of the foundation stiffness correlations described above, the proposed finite element solution implemented in TurbiSoft was applied to nine offshore wind turbines from the literature (Arany et al., 2016; Bakhti et al., 2023; Dj. Amar Bouzid et al., 2018) in order to compute the fixed base natural frequency of each turbine, then drive the natural frequency of the whole system based on the foundation stiffness correlations. The selection of these wind turbines is based on the complete availability of their data. The obtained results are compared with the measured natural frequencies of the whole structure which includes the foundation, the substructure and the tower. The measured natural frequency values have been derived by different signal processing techniques and have been reported by many researchers (Arany et al., 2016). The input parameters of each wind turbine are recapitulated in table 4. Further details on the nine wind turbines can be found in (Arany et al., 2016, 2015; Bakhti et al., 2023).

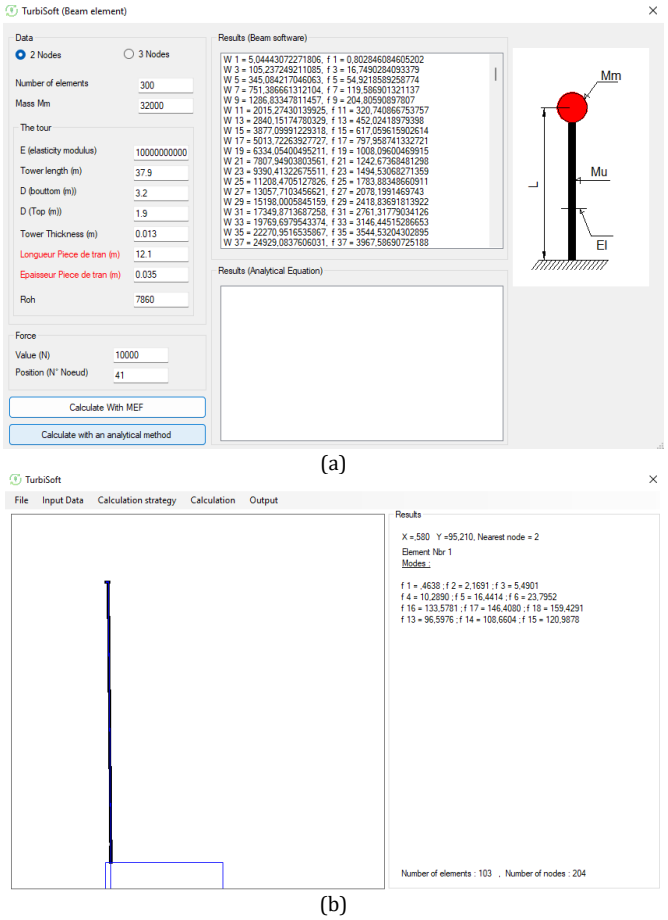

Fig. 5 Screenshots of the computer program TurbiSoft (a): Beam model, (b): Axisymmetric with non-axisymmetric loading model

Table 3. Comparison of the results of the proposed solution with those of other studies for the fixed base model of NREL turbine

Method	Description	Fixed base natural frequency (Hz)
2-node beam elements	Present solution	0.3228
4-node ring element	Present solution	0.3230
8-node ring element	Present solution	0.3212
f_{RB} estimated by You et al. (2022)	ANSYS 2021R1 (3D 20-node element SOLID186)	0.3245
f_{RB} estimated by Yung-Yen Ko (2020)	Analytical model	0.3123
$f_{RB(tapered)}$ estimated by Yung-Yen Ko (2020)	Analytical model	0.3132

Table 4. Input parameters for the nine wind turbines chosen for this analysis

Component dimension	Symbol (unit)	I (Lely)		II (Irene)		III	IV	V	VI	VII
		A2	A3	A	B	Kentish	Barrow	Belwind 1	GunfleetSands	Burbo Bank
Tower height	$L_T\ (m)$	39	39	48.8	48.8	60.06	58	53	60	66
Substructure height	$L_s\ (m)$	12.1	7.1	5.2	6	16.0	33	37	28.0	22.8
Tower top diameter	$D_t\ (m)$	1.9	1.9	1.7	1.7	2.3	2.3	2.3	3.0	3.0
Tower bottom diameter	$D_b\ (m)$	3.2	3.2	3.5	3.5	4.45	4.45	4.3	5.0	5.0
Tower wall thickness	$t_T\ (mm)$	12.0	12.0	13.0	13.0	21.0	32.0	28	33.0	28.0
Substructure wall thickness	$t_s\ (mm)$	35	35	28	28	45.0	70	70	50	45
Monopile diameter	$D_p\ (m)$	3.25	3.7	3.5	3.5	4.45	4.75	5.0	4.7	4.7
Monopile wall thickness	$t_p\ (mm)$	35	35	35	35	45.0	70	70	65	75.0
Monopile embedded length	$L_p\ (m)$	14	21	20	20	18	30	35	38	24
Tower and Monopile Young's modulus	$E_T\ (Gpa)$	210	210	210	210	210	210	210	210	210
Top mass	$m_{RNA}\ (ton)$	32.0	32.0	35.7	35.7	130.8	130.8	130.8	234.5	234.5
Soil's Young's modulus	$E_S\ (Mpa)$	67	72	70	70	60	62	64	81	83
Soil's Poisson's ration	ν	0.4	0.4	0.4	0.4	0.4	0.4	0.4	0.4	0.4

Table 5. Fixed base natural frequencies results

Element	Symbol (unit)	I (A2)	I (A3)	II (A)	II (B)	III	IV	V	VI	VII
8- node axisymmetric (present)	f_{FB}(Hz)	0.7505	0.7999	0.6152	0.6099	0.4074	0.4197	0.4269	0.3765	0.3387
4- node axisymmetric (present)	f_{FB}(Hz)	0.7645	0.8157	0.6265	0.6210	0.4119	0.4255	0.4239	0.3784	0.3410
2D Beam(present)	f_{FB}(Hz)	0.7546	0.8048	0.6177	0.6113	0.4089	0.4225	0.4206	0.3775	0.3427
Measured (whole structure)	f(Hz)	0.634	0.735	0.560	0.546	0.339	0.369	0.372	0.314	0.292

Table 6. Comparison of the measured data with the calculated natural frequencies using proposed finite element models for the tower, and Randolph approach (Randolph, 1981) for the foundation flexibility contribution

Turbine	KL (GN/m)	KLR (GN)	KR (GN m/rad)	CL	CR	Natural frequency (Hz)				Error (%)		
						8 Node (Hz)	4 Node (Hz)	Beam (Hz)	Measured (Hz)	8 Node (%)	4 Node (%)	Beam (%)
I (A2)	5.564	-31.21420	296.94829	0.999837	0.996145214	0.747	0.761	0.751	0.634	17.8	20.1	18.5
I (A3)	6.64	-41.77328	445.25252	0.999864	0.997425857	0.797	0.813	0.802	0.735	8.5	10.68	9.2
II (A)	6.17	-36.91364	374.52177	0.999907	0.996981449	0.613	0.624	0.615	0.56	9.5	11.5	9.9
II (B)	6.17	-36.91364	374.52177	0.999907	0.996981449	0.608	0.619	0.60	0.546	11.3	13.4	11.6
III	7.07	-55.71595	743.74461	0.999851	0.995740312	0.405	0.410	0.407	0.339	19.6	20.9	20.1
IV	7.72	-64.41451	911.17175	0.99977	0.994559328	0.417	0.423	0.420	0.369	13.1	14.6	13.8
V	8.30	-72.38895	1070.29678	0.999773	0.995888546	0.425	0.422	0.418	0.372	14.2	13.4	12.6
VI	9.13	-71.03195	936.91848	0.999714	0.991704805	0.373	0.375	0.374	0.314	18.9	19.5	19.2
VII	9.283	-71.80715	942.02854	0.99982	0.993608011	0.336	0.338	0.340	0.292	15.2	16.0	16.9

Table 7. Comparison of the measured data with the calculated natural frequencies using proposed finite element models for the tower, and Davies & Budhu approach (Davies & Budhu, 1986) for the foundation flexibility contribution

Turbine	K_L (GN/m)	K_{LR} (GN)	K_R (GN m/rad)	C_L	C_R	Natural frequency (Hz)				Error (%)		
						8 Node (Hz)	4 Node (Hz)	Beam (Hz)	Measured (Hz)	8 Node (%)	4 Node (%)	Beam (%)
I (A2)	2.332	-16.65579	207.14538	0.999626	0.94683124	0.746	0.760	0.750	0.634	17.7	19.9	18.3
I (A3)	2.786	-22.29009	310.59954	0.999687	0.996447773	0.797	0.812	0.801	0.735	8.4	10.5	9.1
II (A)	2.586	-19.69700	261.25913	0.999787	0.995835211	0.612	0.623	0.615	0.56	9.4	11.4	9.8
II (B)	2.586	-19.69700	261.25913	0.999787	0.995835211	0.607	0.618	0.608	0.546	11.2	13.2	11.5
III	2.967	-29.72985	518.82184	0.999656	0.994125553	0.405	0.409	0.406	0.339	19.4	20.7	19.9
IV	3.237	-34.37138	635.61578	0.999471	0.992500254	0.416	0.422	0.419	0.369	12.8	14.4	13.6
V	3.480	-38.62651	746.61832	0.999478	0.994329658	0.424	0.421	0.418	0.372	14.0	13.2	12.4
VI	3.828	-37.90242	653.57619	0.999343	0.988577815	0.372	0.374	0.373	0.314	18.4	19.5	18.8
VII	3.891	-38.31606	657.14087	0.999587	0.99119209	0.335	0.338	0.339	0.292	14.9	15.7	16.3

Table 8. Comparison of the measured data with the calculated natural frequencies using proposed finite element models for the tower, and DNV approach (DNV-OS-J101, 2014) for the foundation flexibility contribution

Turbine	K_L (GN/m)	K_{LR} (GN)	K_R (GN m/rad)	C_L	C_R	Natural frequency (Hz)				Error (%)		
						8 Node (Hz)	4 Node (Hz)	Beam (Hz)	Measured (Hz)	8 Node (%)	4 Node (%)	Beam (%)
I (A2)	2.186	-15.06527	201.72908	0.99965	0.995207564	0.746	0.760	0.751	0.634	17.7	19.9	18.4
I (A3)	2.608	-20.09633	301.97788	0.999707	0.99680555	0.797	0.813	0.802	0.735	8.4	10.6	9.1
II (A)	2.423	-17.78098	254.17171	0.999801	0.996251332	0.612	0.624	0.615	0.56	9.4	11.4	9.8
II (B)	2.423	-17.78098	254.17171	0.999801	0.996251332	0.607	0.618	0.609	0.546	11.2	13.3	11.5
III	2.786	-27.02470	506.54001	0.999677	0.994687056	0.405	0.409	0.406	0.339	19.5	20.8	19.9
IV	3.039	-31.19783	620.10129	0.999504	0.993222788	0.417	0.422	0.419	0.369	12.9	14.4	13.6
V	3.265	-35.01003	727.86272	0.99951	0.994881762	0.424	0.421	0.418	0.372	14.1	13.3	12.4
VI	3.577	-33.99149	633.71509	0.999389	0.989755112	0.372	0.374	0.373	0.314	18.6	19.2	18.9
VII	3.634	-34.32475	636.81409	0.999616	0.992107608	0.336	0.338	0.340	0.292	15.0	15.8	16.4

Table 9. Comparison of the measured data with the calculated natural frequencies using proposed finite element models for the tower, and Higgins approach (Higgins et al., 2013) for the foundation flexibility contribution

Turbine	K_L (GN/m)	K_{LR} (GN)	K_R (GN m/rad)	C_L	C_R	Natural frequency (Hz)				Error (%)		
						8 Node (Hz)	4 Node (Hz)	Beam (Hz)	Measured (Hz)	8 Node (%)	4 Node (%)	Beam (%)
I (A2)	3.985	-39.14426	488.26143	0.999561	0.99547673	0.747	0.761	0.750	0.634	17.8	20.0	18.4
I (A3)	8.560	-126.8199	2295.56813	0.999761	0.99886982	0.799	0.814	0.803	0.735	8.7	10.8	9.3
II (A)	7.982	-112.64148	1940.25359	0.999838	0.99867508	0.614	0.625	0.617	0.56	9.7	11.7	10.1
II (B)	7.982	-112.64148	1940.25359	0.999838	0.99867508	0.609	0.620	0.610	0.546	11.5	13.6	11.8
III	4.297	-54.20434	875.87614	0.99954	0.99325318	0.404	0.409	0.406	0.339	19.3	20.6	19.7
IV	11.770	-249.62704	6372.75380	0.999634	0.99810678	0.418	0.424	0.4215	0.369	13.5	15.0	14.2
V	15.776	-391.17293	11507.7557	0.999688	0.99899845	0.426	0.423	0.420	0.372	14.6	13.8	12.9
VI	25.187	-680.00247	21347.0251	0.999696	0.99892499	0.376	0.378	0.377	0.314	19.7	20.3	20.0
VII	10.103	-170.69177	3576.15047	0.99965	0.99642037	0.3376	0.339	0.3413	0.292	15.5	16.3	16.9

The beam element and the volume element models used in this solution give quite close natural frequency results as shown in table 5. It can be seen that there is no significant difference between the two natural frequency estimation models (less than 2%). Furthermore, these models provide an important reduction in computational effort compared with the three-dimensional numerical model. The axisymmetric model (under non-axisymmetric loading) is advantageous because its application isn't limited to the tower only, but it can be used also for modelling the whole system of the foundation as demonstrated by Bakhti et al (2023), where the error margin in the estimation of the natural frequency of the selected nine offshore wind turbines was less than 3.5 %.

Tables 6, 7, 8, and 9 show the natural frequency of the whole system of the selected nine offshore wind turbines using the proposed finite element models for the tower and the four analytical correlation formulas

for the foundation flexibility contribution. Obtained results indicated that, whatever the finite element model used for the tower, the error margin in the estimation of the natural frequency of the whole system is between 9% and 20 % compared to the measured ones for the four used correlation formulas. This significant error is attributed to the low accuracy of these four correlation formulas for predicting the foundation flexibility contribution, because the natural frequency of the whole system was estimated by the authors in (Bakhti et al., 2023) through this finite element model, and the error margin of the same turbines was less than 3.5 %. The results from the four correlation formulas used are quite similar, with a difference in the error margin of less than 1%. However, the largest error margins are observed with the Higgins formula (Higgins et al., 2013), which has been originally developed for short monopiles, even though the analyzed monopiles can be considered short, with monopile slenderness ratios less than 8. More research work is required to improve the accuracy of the foundation flexibility contribution prediction equations.

7. Conclusion

The evaluation of natural frequency of the wind turbine is a crucial step in the design calculation to avoid resonance phenomena. In this paper, a study of the impact of foundation stiffness correlations on the natural frequency of the whole system has been conducted. A finite element solution has been proposed in which the fixed base natural frequencies of the wind turbines are estimated using two finite element models for the tower modelling: beam and volume model. One type of beam element and two types of volume element have been used; 2-node beam elements, 4-node ring and 8-node ring. This solution has been coded in a special-purpose computer program TurbiSoft in which the natural frequency of fixed base wind turbines is provided. Obtained results from the proposed solution indicate that the natural frequency estimates of the fixed-base wind turbine are reasonably accurate and reliable. It is observed from the analysis of a 5.0 MW offshore wind turbine model provided by the NREL that the natural frequency of the fixed base model, as calculated using the two proposed approaches, deviates by approximately 1-4% from that of Yung-Yen and You et al. The calculation of the natural frequency of the whole system of nine wind turbines is carried out using the proposed finite element solution to compute their fixed base natural frequencies, and the foundation flexibility correlations to estimate the contribution of the foundation. Four correlation formulas for foundation flexibility are used, namely that of Randolph, Davies and Budhu, DNV, and Higgins. Obtained results indicate that the estimated error margin for the natural frequencies of the entire structures is between 9-20%, which represents an important value compared to the measured frequencies. The large values of the error margin compared to numerical studies in the literature demonstrate the low accuracy of these four correlation formulas for predicting the foundation flexibility contribution. The results from the four correlation formulas used are quite similar, with a difference in the error margin of less than 1%. However, the largest error margins are observed with the Higgins formula, which has been originally developed for short monopiles, even though the analyzed monopiles can be considered short, with monopile slenderness ratios less than 8. More research work is required to improve the accuracy of the foundation flexibility contribution prediction equations.

Abbreviations

RNA: rotor nacelle assembly
NREL: National Renewable Energy Laboratory

References

A. Abdullahi and Y. Wang. 2021. "Digital Twin-like Model Updating of a Laboratory Offshore Wind Turbine with Few-Parameters Soil-Structure Interaction Model." SHMII 10 Porto, Portugal: Proceedings of the 10th International Conference on Structural Health Monitoring of Intelligent Infrastructure.

Adhikari, S., and S. Bhattacharya. 2012. "Dynamic Analysis of Wind Turbine Towers on Flexible Foundations." Shock and Vibration, 19 (1): 37–56. https://doi.org/10.1155/2012/408493.

Alkhoury, P., A. Soubra, V. Rey, and M. Aït-Ahmed. 2021. "A full three-dimensional model for the estimation of the natural frequencies of an offshore wind turbine in sand." Wind Energy, 24 (7): 699–719. https://doi.org/10.1002/we.2598.

Arany, L., S. Bhattacharya, S. Adhikari, S. J. Hogan, and J. H. G. Macdonald. 2015. "An analytical model to predict the natural frequency of offshore wind turbines on three-spring flexible foundations using two different beam models." Soil Dynamics and Earthquake Engineering, 74: 40–45. https://doi.org/10.1016/j.soildyn.2015.03.007.

Arany, L., S. Bhattacharya, J. H. G. Macdonald, and S. J. Hogan. 2016. "Closed form solution of Eigen frequency of monopile supported offshore wind turbines in deeper waters incorporating stiffness of substructure and SSI." Soil Dynamics and Earthquake Engineering, 83: 18–32. https://doi.org/10.1016/j.soildyn.2015.12.011.

Bakhti, R., B. Benahmed, and A. Laib. 2024. "Finite Element Investigation of Offshore Wind Turbines Natural Frequency with Monopile Foundations System." J. Vib. Eng. Technol., 12 (2): 2437–2449. https://doi.org/10.1007/s42417-023-00989-3.

Blevins, R. D. 2001. Formulas for natural frequency and mode shape. Malabar, Florida: Krieger Publishing.

Davies, T. G., and M. Budhu. 1986. "Non-linear analysis of laterally loaded piles in heavily overconsolidated clays." Géotechnique, 36 (4): 527–538. https://doi.org/10.1680/geot.1986.36.4.527.

Dj. Amar Bouzid, R. Bakhti, and S. Bhattacharya. 2018. "The dynamics of an offshore wind turbine using a FE semi-analytical analysis considering the interaction with three soil profiles."

DNV-OS-J101. 2014. "Design of offshore wind turbine structures." Oslo, Norway.

Higgins, W., C. Vasquez, D. Basu, and D. V. Griffiths. 2013. "Elastic Solutions for Laterally Loaded Piles." J. Geotech. Geoenviron. Eng., 139 (7): 1096–1103. https://doi.org/10.1061/(ASCE)GT.1943-5606.0000828.

Huang, H. S. 2022. "Simulations of 10MW wind turbine under seismic loadings." Composite Structures, 279: 114686. https://doi.org/10.1016/j.compstruct.2021.114686.

J.H Vught. 2000. "Considerations on the dynamics of support structures for an offshore wind energy converter." Ph.D thesis. The Netherlands: Delft University of Technology.

Kaiser, H. F. 1972. "The JK method: a procedure for finding the eigenvectors and eigenvalues of a real symmetric matrix." The Computer Journal, 15 (3): 271–273. https://doi.org/10.1093/comjnl/15.3.271.

Ko, Y.-Y. 2020. "A simplified structural model for monopile-supported offshore wind turbines with tapered towers." Renewable Energy, 156: 777–790. https://doi.org/10.1016/j.renene.2020.03.149.

Owji, R., G. Habibagahi, and M. Veiskarami. 2023. "Effects of Cyclic and Post-cyclic Loading on Lateral Response of Flexible Piles Embedded in Dry Sand." Int J Civ Eng, 21 (4): 633–645. https://doi.org/10.1007/s40999-022-00790-5.

Park, G., D. You, K.-Y. Oh, and W. Nam. 2022. "Natural Frequency Degradation Prediction for Offshore Wind Turbine Structures." Machines, 10 (5): 356. https://doi.org/10.3390/machines10050356.

Randolph, M. F. 1981. "The response of flexible piles to lateral loading." Géotechnique, 31 (2): 247–259. https://doi.org/10.1680/geot.1981.31.2.247.

Rong, X.-N., R.-Q. Xu, H.-Y. Wang, and S.-Y. Feng. 2017. "Analytical solution for natural frequency of monopile supported wind turbine towers." Wind and Structures, 25 (5): 459–474. https://doi.org/10.12989/WAS.2017.25.5.459.

Seo, Y.-H., M. S. Ryu, and K.-Y. Oh. 2020. "Dynamic Characteristics of an Offshore Wind Turbine with Tripod Suction Buckets via Full-Scale Testing." Complexity, 2020: 1–16. https://doi.org/10.1155/2020/3079308.

Shi, S., E. Zhai, C. Xu, K. Iqbal, Y. Sun, and S. Wang. 2022. "Influence of Pile-Soil Interaction on Dynamic Properties and Response of Offshore Wind Turbine with Monopile Foundation in Sand Site." Applied Ocean Research, 126: 103279. https://doi.org/10.1016/j.apor.2022.103279.

Steinacker, H., F. Lemmer, S. Raach, D. Schlipf, and P. W. Cheng. 2022. "Efficient multibody modeling of offshore wind turbines with flexible substructures." J. Phys.: Conf. Ser., 2265 (4): 042007. https://doi.org/10.1088/1742-6596/2265/4/042007.

Van Der Tempel, J., and D.-P. Molenaar. 2002. "Wind Turbine Structural Dynamics – A Review of the Principles for Modern Power Generation, Onshore and Offshore." Wind Engineering, 26 (4): 211–222. https://doi.org/10.1260/030952402321039412.

Xu, Y., G. Nikitas, T. Zhang, Q. Han, M. Chryssanthopoulos, S. Bhattacharya, and Y. Wang. 2020. "Support condition monitoring of offshore wind turbines using model updating techniques." Structural Health Monitoring, 19 (4): 1017–1031. https://doi.org/10.1177/1475921719875628.

You, Y.-S., K.-Y. Song, and M.-Y. Sun. 2022. "Variable Natural Frequency Damper for Minimizing Response of Offshore Wind Turbine: Principal Verification through Analysis of Controllable Natural Frequencies." JMSE, 10 (7): 983. https://doi.org/10.3390/jmse10070983.

Disclaimer